

The Effect of Nearest Neighbor [Pb-O] Divacancy Pairs on the Ferroelectric-Relaxor Transition in Nano-Ordered $\text{Pb}(\text{Sc}_{1/2}\text{Nb}_{1/2})\text{O}_3$

B. P. Burton¹, Silvia Tinte¹, Eric Cockayne¹, U. V. Waghmare²

¹Ceramics Division,
Materials Science and Engineering Laboratory,
National Institute of Standards and Technology
Gaithersburg, MD 20899-8520, USA
Email: benjamin.burton@nist.gov

²J. Nehru Theoretical Sciences Unit, JNCASR,
Jakkur, Bangalore, 560 064, INDIA

Molecular dynamics simulations were performed on a first-principles-based effective Hamiltonians for chemically short-range ordered $\text{Pb}(\text{Sc}_{1/2}\text{Nb}_{1/2})\text{O}_3$ with nearest neighbor [Pb-O] divacancy pairs. The divacancy-concentration ($X_{[\text{Pb-O}]}$) vs. temperature phase diagram was calculated, and it is topologically equivalent to the hydrostatic pressure (P) vs. temperature diagram: a ferroelectric ground-state phase at low $X_{[\text{Pb-O}]}$ (P); that transforms to a relaxor paraelectric phase at moderate $X_{[\text{Pb-O}]}$ (P); followed by a crossover to a normal paraelectric phase at high $X_{[\text{Pb-O}]}$ (P).

Keywords: PSN; Relaxor Ferroelectric; lead vacancies; oxygen vacancies; phase transitions; random fields

INTRODUCTION

Chemically disordered $\text{Pb}(\text{Sc}_{1/2}\text{Nb}_{1/2})\text{O}_3$ (PSN) exhibits a relaxor ferroelectric (RFE [1,2]) to normal ferroelectric (FE) transition; and Chu et al. [3] demonstrated that the addition of 1.7 atomic percent [Pb-O] divacancy pairs depresses the FE transition temperature (T_{FE}) of chemically disordered PSN from $\approx 373\text{K}$ to $\approx 338\text{K}$. Chu et al. also reported similar and more complete results for isostructural $\text{Pb}(\text{Sc}_{1/2}\text{Ta}_{1/2})\text{O}_3$ (PST) [4-6]. These results suggest that a sufficient concentration of divacancy pairs, $X_{[\text{Pb-O}]}$, will drive the system to a fully relaxor state, that has no FE ground-state phase. Introducing Pb-vacancies [7], or [Pb-O] divacancy pairs [8] increases the average strength of local "random fields" $\langle \mathbf{h}_i \rangle$, ($\langle \dots \rangle$ indicates spatial statistical averaging) [9,10] that, at sufficient $X_{[\text{Pb-O}]}$ yield a fully relaxor state. Thus, $\langle \mathbf{h}_i \rangle$ can be regarded as a *nonordering* field [11] that tunes the proportions of RFE and FE character in the system.

Increasing hydrostatic pressure (P) drives chemically disordered PSN into a fully relaxor state [12] and the results of previous simulations by Tinte et al. [9] convincingly explain this as follows: 1) P has a negligible effect on $\langle \mathbf{h}_i \rangle$; 2) P smoothly and monotonically reduces FE well depths [13-15] and thus destabilizes the FE phase relative to the RFE state of the paraelectric (PE) phase; 3) Keeping $\langle \mathbf{h}_i \rangle$ constant while reducing FE well depth corresponds to an *indirect relative increase* in $\langle \mathbf{h}_i \rangle$. Because P *indirectly* increases $\langle \mathbf{h}_i \rangle$, it will only induce a FE-RFE

transition in a sample that has some RFE character even at $P=0$ (e.g. chemically disordered PSN). In a sample without significant $\langle \mathbf{h}_i \rangle$ (e.g. PSN with perfect chemical order) moderate pressure induces a FE-PE transition [16] without RFE character. Increasing $X_{[\text{Pb-O}]}$, *directly* increases $\langle \mathbf{h}_i \rangle$, and drives the system towards a FE-RFE transition, even if $\langle \mathbf{h}_i \rangle = 0$ initially (e.g. PSN with perfect chemical order has $\langle \mathbf{h}_i \rangle = 0$).

COMPUTATIONAL METHODS

Simulations were performed using the first-principle effective Hamiltonian, H_{eff} , which is described in detail in [10]; H_{eff} is an expansion of the potential energy of PSN in a Taylor series about a high-symmetry perovskite reference structure. It includes those degrees of freedom relevant to ferroelectric phase transitions:

$$H_{\text{eff}} = H(\{\xi_i\}) + H(e_{\alpha\beta}) + H(\{\xi_i\}, \epsilon_{\alpha\beta}) + PV + H(\{\xi_i\}, \{\sigma_i\}, \{[\text{Pb-O}]\})$$

where ξ_i represents Pb-site centered local polar distortion variables; $e_{\alpha\beta}$ is the homogeneous strain term; $H(\{\xi_i\}, e_{\alpha\beta})$ is a strain coupling term; and PV the standard pressure-volume term. The first four terms are sufficient to model pressure-dependent phase transitions in a normal FE perovskite [17]. The fifth term, $H(\{\xi_i\}, \{\sigma_i\}, \{[\text{Pb-O}]\})$, represents coupling between polar variables and "random" local fields, $\langle \mathbf{h}_i \rangle$ [10,18,19] from: 1) screened electric fields from the quenched distribution of Sc^{3+} and Nb^{5+} ions (σ_i); and 2) randomly distributed nearest neighbor (NN) Pb-O divacancy pairs, $[\text{Pb-O}]$.

Further details of the simulations used to calculate Figures 2 are given in: the review by Burton et al. [10]; the study of P-effects [9]; and the first-principles calculation of the dipole moment for a $[\text{Pb-O}]$ NN divacancy pair in PbTiO_3 [8]. In Tinte et al [9] the simulation supercell contained $40 \times 40 \times 40$ Pb-site local mode variables in a "nano-ordered" chemical configuration of 20 ordered 800-site clusters, in a percolating random matrix which (for accounting purposes only) was subdivided into 60 disordered clusters. The same simulation cell is used here, except that $(40^3)X_{[\text{Pb-O}]}$ randomly selected local mode variables are replaced by dipole moments corresponding to NN $[\text{Pb-O}]$ divacancy pairs. This treatment is distinct from Bellaiche et al. [7] which considered $[\text{Pb}]$ -vacancies without charge-compensating $[\text{O}]$ -vacancies; presumably the real system has both $[\text{Pb}]$ - and $[\text{O}]$ -vacancies as reported by Chu et al. [3].

RESULTS AND DISCUSSION

The simulations predict a significantly steeper slope for the FE-RFE transition than is observed experimentally. A possible explanation is that the populations of second- and possibly farther-neighbor divacancy pairs are significant, and that a realistic representation would include local electric fields induced by $[\text{Pb}]$ - and $[\text{O}]$ -vacancies and by closely bound $[\text{Pb-O}]$ divacancy pairs. In fact, Vienna abinitio simulation package with projector augmented wave potentials and a generalized gradient approximation for the exchange/correlation potential [20] calculations for NN and next-NN (NNN) $[\text{Pb-O}]$ divacancy pairs in a $2 \times 2 \times 2$ supercell (40 atoms for PSN; 38 atoms with a divacancy) indicate that NNN divacancies are actually ≈ 0.016 eV lower in energy than NN divacancies (Fig. 1; Table 1).

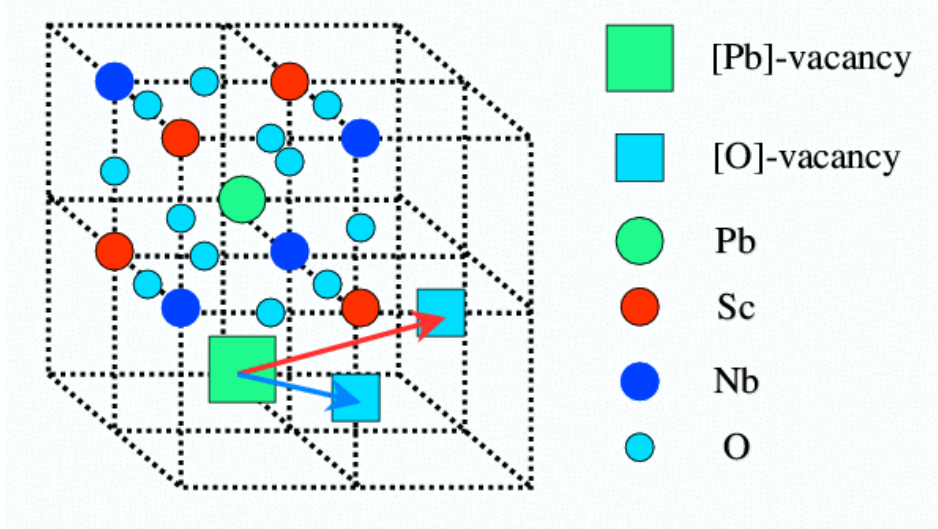


Figure 1: Representation of the 2x2x2 perovskite supercell for chemically ordered $Pb_8(Sc_4Nb_4)O_{24}$ and the $Pb_7(Sc_4Nb_4)O_{23}$ supercells with nearest- and next-nearest neighbor divacancy pairs. Atoms are only shown in 1/8 of the supercell.

There are two plausible relations from which to estimate formation energies for the NN and NNN divacancy pairs:

1. $\Delta E_f = E(Pb_7Sc_4Nb_4O_{23}) + E(\alpha-PbO) - E(Pb_8Sc_4Nb_4O_{24})$.
2. $\Delta E_f = E(Pb_7Sc_4Nb_4O_{23}) - (7/8)E(Pb_8Sc_4Nb_4O_{24}) - (1/2)E(ScNbO_4)$

Initial structures for $\alpha-PbO$ and Wolframite-structure $ScNbO_4$ were taken from [21] and [22] respectively (the $CdWO_4$ structure in their Table II). Monkhorst-Pack k-point meshes were used: 10x10x8 $\alpha-PbO$; 6x6x6 $ScNbO_4$; 4x4x4 for $Pb_8Sc_4Nb_4O_{24}$ and $Pb_7Sc_4Nb_4O_{23}$ supercells. All calculations were done with an energy cutoff of 500 eV, and all were fully relaxed. The (very similar) results from both are listed in Table 1 with corresponding volumes of formation, ΔV_f .

Table 1: Formation energies and formation volumes of nearest- and next-nearest-neighbor [Pb-O] divacancy pairs in a chemically ordered $Pb_8Sc_4Nb_4O_{24}$ supercell.

System	Relation 1		Relation 2	
	ΔE_f (eV)	ΔV_f (\AA^3)	ΔE_f (eV)	ΔV_f (\AA^3)
NN [Pb-O] divacancy	1.54	37.6	1.51	43.6
NNN [Pb-O] divacancy	1.40	34.9	1.38	40.8

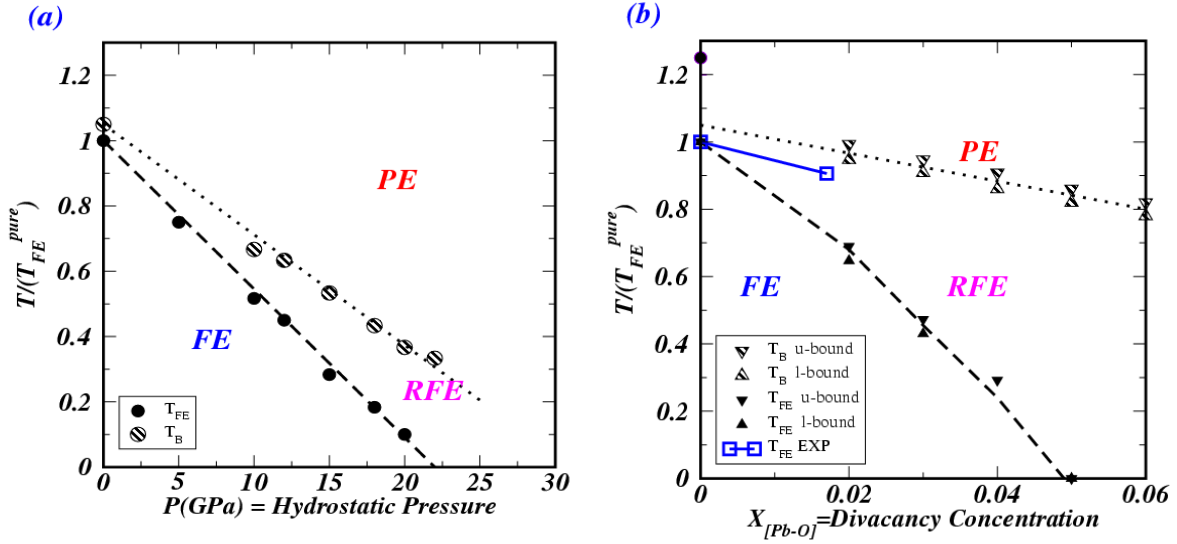


Figure 2: Predicted PSN phase diagrams: (a) pressure vs. reduced temperature [9]; (b) [Pb-O] divacancy concentration vs. reduced temperature. Dashed lines indicate ferroelectric-relaxor transitions. Dotted lines indicate Burns temperatures, T_B [23]. Triangles indicate upper- and lower-bounds, u- and l- respectively. The diagrams are topologically equivalent because both P and $X_{[Pb-O]}$ tune the delicate balance between FE well depth (increasing P reduces well depths) and the spatial average strength of the "random fields," $\langle h_i \rangle$, that promote the relaxor state.

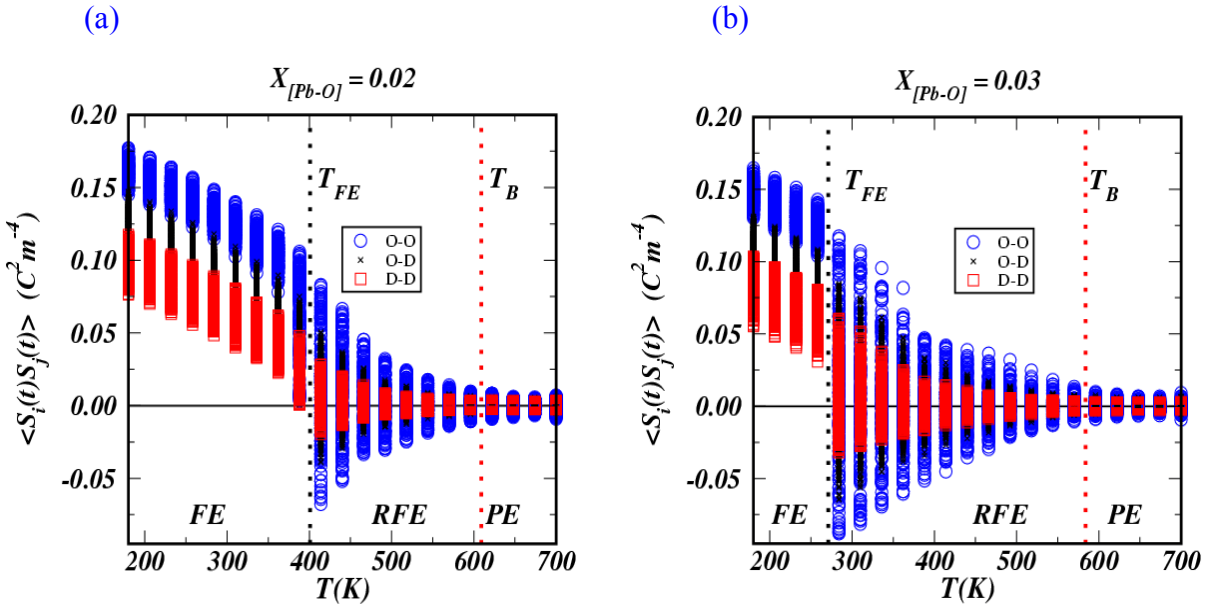


Figure 3: Predicted cluster-cluster spin products for a nano-ordered system with (a) $X_{[Pb-O]} = 0.02$ and (b) $X_{[Pb-O]} = 0.03$. Vertical lines indicate T_{FE} and T_B , the ferroelectric transition temperature and the Burns temperature [20], respectively. Increasing $X_{[Pb-O]}$ increases the relaxor interval and, drives the ferroelectric-relaxor transition to lower temperature.

The results presented in Table 1 indicate that our NN divacancy approximation is an oversimplification, because $\Delta E_f(\text{NN}) > \Delta E_f(\text{NNN})$. Thus, a realistic treatment would at least include about equal concentrations of NN- and NNN-divacancies, and probably isolated [Pb] and [O] vacancies as well, with the precise distribution depending on temperature. That said, there is no obvious reason to believe that a more realistic model for the vacancy distribution would yield qualitatively different results.

Calculated P vs. T/T_{FE} and $X_{[\text{Pb-O}]}$ vs. T/T_{FE} diagrams are plotted in Figs. 2a and 2b, respectively. Dashed lines indicate FE-RFE transitions, and dotted lines indicate Burns temperatures, T_B [20]. Qualitatively, the only apparent (small) difference between Figures 2a and 2b is that the RFE-FE transition in Fig. 2a is approximately linear, while in Fig. 2b it exhibits slight negative curvature.

As in the P-dependent simulations, cluster-cluster spin products were calculated for 800-site clusters (Figs. 3): O-O are the products between average spins on two chemically ordered clusters; O-D are products between one chemically ordered and one chemically disordered cluster; and D-D the products between two chemically disordered clusters. These results are analogous to those from P-dependent simulations, in that they exhibit the same hierarchy of correlations: O-O > O-D > D-D. Also, as $X_{[\text{Pb-O}]}$, and therefore $\langle h_i \rangle$, is increased, the RFE-state region grows, mostly at the expense of the FE-phase.

CONCLUSIONS

Directly increasing local “random fields”, $\langle h_i \rangle$, by increasing $X_{[\text{Pb-O}]}$, enlarges the RFE-state region and ultimately drives the system into a fully relaxor state. This progression mirrors the phenomenology of PSN under increasing hydrostatic pressure. The essential difference is that $X_{[\text{Pb-O}]}$ *directly* increases $\langle h_i \rangle$, whereas increasing pressure makes FE well depths shallower, which corresponds to an thus *indirect* increase in $\langle h_i \rangle$, relative to FE well depth.

REFERENCES

- [1] G.A. Smolensky and A. I. Agranovskaya, Sov. Phys. Sol. State **1**, 1429 (1959).
- [2] L. E. Cross, Ferroelectrics **76**, 241 (1987).
- [3] F. Chu, I.M. Reaney and N. Setter, J. Appl. Phys. **77**[4], 1671 (1995).
- [4] F. Chu, N. Setter and A. K. Tagantsev, J. Appl. Phys. **74**[8], 5129 (1993).
- [5] F. Chu, I.M. Reaney and N. Setter, J. Amer. Ceram. Soc. **78**[7], 1947 (1995).
- [6] F. Chu, G. Fox and N. Setter, J. Amer. Ceram. Soc. **81**(6) 1577 (1998).
- [7] L. Bellaiche, J. Iniguez, E. Cockayne, and B. P. Burton Phys. Rev. B **75**, 014111 (2007).
- [8] E. Cockayne and B. P. Burton, Phys. Rev. B **69**, 144116 (2004).
- [9] S. Tinte, B. P. Burton, E. Cockayne and U. V. Waghmare, Phys. Rev. Lett. **97**, 137601 (2006).
- [10] B. P. Burton, E. Cockayne, S. Tinte and U. V. Waghmare, Phase Trans. **79**, 91 (2006).
- [11] J. M. Kosterlitz, D. R. Nelson and M. E. Fisher Phys. Rev. B, **13** 412- (1976). "A nonordering field [\mathbf{g}] alters nonuniversal critical parameters, like critical-point energies specific heat, and spontaneous order amplitudes, but does *not* change the basic nature of the critical point so that, in particular, universal quantities such as critical exponents do not vary with \mathbf{g} ".
- [12] E. L. Venturini, R. K. Grubbs, G. A. Samara, Y. Bing and Z.-G. Ye, Phys. Rev. B **74**, 064108 (2006).

- [13] R. E. Cohen, Nature (London) 358, 137 (1992), Also, R.E. Cohen and H. Krakauer, Ferroelectrics **136**, no.1-4, 65 (1992)
- [14] G. Saghi-Szabo, R. E. Cohen and H. Krakauer, Phys. Rev. Lett. **80**, 4321 (1998).
- [15] M. Fornari and D. Singh Phys. Rev. B **63**, 092101 (2001).
- [16] G. A. Samara, Phys. Rev. Lett. **77**, 314 (1996); J. Appl. Phys. **84**, 2538 (1998); in *Fundamental Physics of Ferroelectrics 2000*, edited by R. E. Cohen (American Institute of Physics, New York, 2000), p. 344; J. Phys.: Condens. Matter **15**, R367 (2003).
- [17] W. Zhong, D. Vanderbilt and K. M. Rabe, Phys. Rev. Lett. **73**, 1861 (1994); K. M. Rabe and U. V. Waghmare, Phys. Rev. B **52**, 13236 (1995); U. V. Waghmare and K. M. Rabe, Phys. Rev. B **55**, 6161 (1997).
- [18] U. V. Waghmare, E. Cockayne, and B. P. Burton, Ferroelectrics **291**, 187 (2003).
- [19] B. P. Burton, U. V. Waghmare and E. Cockayne, TMS Letters, **1**, 29 (2004).
- [20] G. Kresse and J. Hafner, Phys. Rev. B **47**, RC558 (1993); G. Kresse, Thesis, Technische Universitat Wien, 1993; G. Kresse and J. Furthmuller, Comput. Mat. Sci. **6**, 15 (1996); G. Kresse and J. Furthmuller, Phys. Rev. B **54**, 11169 (1996). (Note: The identification of any commercial product or trade name does not imply endorsement or recommendation by the National Institute of Standards and Technology).
- [21] G. W. Watson, S.C. Parker and G. Kresse, Phys. Rev. B **59**, 8481 (1999)
- [22] Y. Abarham, N. A. W. Holzwarth and R. T. Williams Phys. Rev. B **62**, 1733 (2000)
- [23] G. Burns and F. H. Dacol, Solid State Commun. **48**, 853 (1983).